

**DETC2005/VIB-85391**

## DISTRIBUTION OF SUB AND SUPER HARMONIC SOLUTION OF MATHIEU EQUATION WITHIN STABLE ZONES

G. Nakhaie Jazar, Reza.N.Jazar@ndsu.edu

Mahinfalah, M., M.Mahinfalah@ndsu.edu

M. Rastgaar Aagaah, Aagaah.Rastgaar@ndsu.edu

N. Mahmoudian, Nina.Mahmoudian@ndsu.edu

Dept. of Mech. Eng. North Dakota State University, Fargo, 58105-5285, USA

**KEYWORDS:** Mathieu equation dynamics, Sub and super-harmonics oscillation, Parametric vibrations.

### Abstract

The third stable region of the Mathieu stability chart, surrounded by one  $\pi$ -transition and one  $2\pi$ -transition curve is investigated. It is known that the solution of Mathieu equation is either periodic or quasi-periodic when its parameters are within stable regions. Periodic responses occur when they are on a "splitting curve". Splitting curves are within stable regions and are corresponding to coexisting of periodic curves where an instability tongue closes. Distributions of sub and super-harmonics, as well as quasi-periodic solutions are analyzed using power spectral density method.

### 1. INTRODUCTION

Stability diagram for the angular Mathieu equation

$$\ddot{x} + a \cdot x - 2b \cdot x \cdot \cos(2t) = 0 \quad \dot{x} = \frac{dx}{dt} \quad (1)$$

is depicted in Figure 1 [1]. The stability diagram is developed by plotting relationship between constant parameters  $a$  and  $b$  for  $\pi$  and  $2\pi$ -periodic solutions of Mathieu Equation [2]. The parameters  $a$  and  $b$  are called control parameters simply because they control dynamic behavior of the equation. More specifically, depending on the value of  $a$  and  $b$ , response of the equation can be periodic, quasi-periodic, or unstable. The stability chart is made by plotting the curves called transition curves which indicate the boundary of stable and unstable regions [3-10].

In Figure 1, each stable zone is bounded by two transition curves starting off the horizontal axes, from integer roots of equation  $a - n^2 = 0$ ,  $n=0, 1, 2, 3, \dots$ . We name the stable zones as *first*, for the zone bounded between transient curves started from  $a=0, 1$ ; *second*, for the zone bounded between transient curves started from  $a=1, 4$ , and so on. The *third* stable zone, which is bounded between curves starting from  $a=4$  and  $a=9$ , will be examined in this paper as an example.

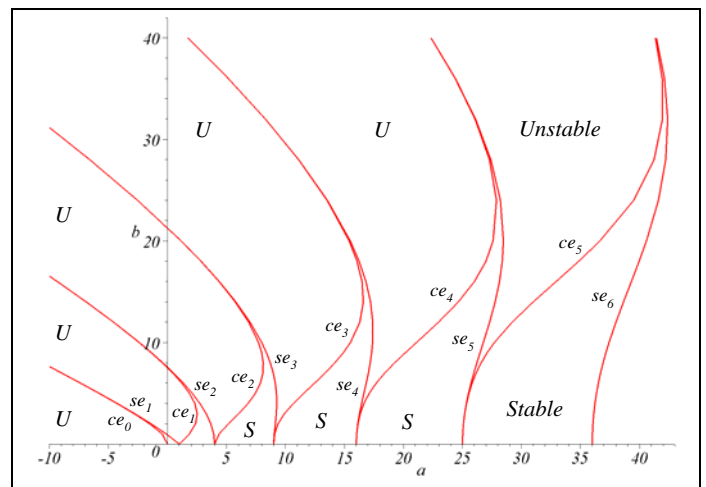


**Figure 1.** Mathieu stability diagram based on the numerical values, generated by McLachlan (1947).

Power spectral density for time response of the equation is utilized to determine the general behavior of the

system. This investigation also indicates how we may find the splitting (or coexistence) curves within each stable zone. In addition, applying energy-rate method provides a geometrical illustration of the stability within each region.

## 2. THE THIRD STABLE ZONE

Applying Energy-Rate method [11], an illustration of three dimensional view of  $2\pi$ -Mathieu stability surface in the third stable zone is shown in Figure 2. Contours of Energy-Rate of the  $2\pi$ -stability surface are plotted in Figure 3.

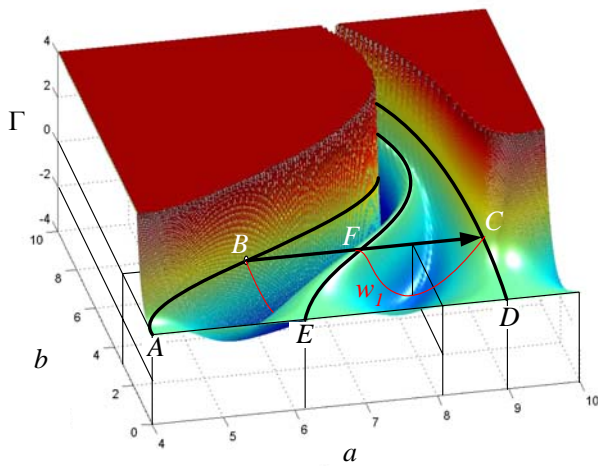


**Figure 2.** The third stability zone of  $2\pi$ -stability surface of Mathieu equation

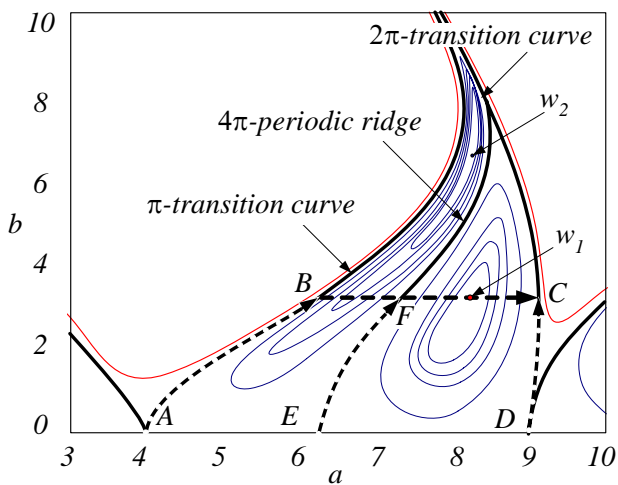


**Figure 3.** Contours of Energy-Rates in the third stability zone for  $2\pi$ -stability surface of Mathieu equation

Time integral of an equation of motion over a period for a periodic solution must be zero. Since Mathieu equation has periodic solution on transition curves, its time integral would be zero on these curves, while it is equal to a positive number for a point in unstable region and a negative number for a point within a stable region. Evaluating time integral of Mathieu equation,  $\Gamma$ , over  $2\pi$  for a domain of parametric plane can determine the stable and unstable regions, as well as splitting lines.

Skew symmetry characteristic of Mathieu equation implies the  $2T$ -periodic transition curves will also appear when Energy-Rate is applied on  $T$ -periodic function [11]. Therefore, the ridge in Figure 2 indicates a  $4\pi$ -periodic splitting curves [9]. As a result, zero level line of the left wall of the stable valley in Figure 2 is a  $1$  to  $1$  or  $\pi$ -periodic transition, while the zero level line of the right wall of the third stable valley is a  $2$  to  $1$  or  $2\pi$ -periodic transition curve.

It is seen in Figure 2, that there are two wells  $w_1$  and  $w_2$  in the stable valley at points  $(a_1=8.192, b_1=3.084)$  and  $(a_2=8.198, b_2=7.04)$ . The dividing ridge touches the zero level plane and indicates a  $4\pi$ -periodic curve.

In order to investigate the behavior of Mathieu equation in the third stable region, we will walk along a path from point B on the  $\pi$ -transition wall to point C on  $2\pi$ -transition wall passing over  $w_1$ . We will also analyze the behavior of the equation on the  $\pi$  and  $2\pi$ -transition curves as well as the  $4\pi$ -periodic ridge. The two and three dimensional illustration of the paths of investigation are shown in Figures 2 and 3.

**Table 1.** Characteristics of point 0 to 4

point	$b$	$a$
4	3.084	9.228
3	3.084	8.192
2	3.084	7.205
1	3.084	6.417
0	3.084	6.116

We study the Mathieu equations on 5 different points on the line  $b=3.084$ , corresponding to the path B-C. Point 0 is on the  $\pi$ -transition curve, while point 1 is an arbitrary investigating points between the  $\pi$ -transition curve and the  $4\pi$ -periodic ridge at local minimum. Point 2 is on the

$4\pi$ -periodic ridge. Point 3 is corresponding to the well  $w_j$ , and point 4 is an investigating point on the  $2\pi$ -transition curve of Mathieu stability diagram. The information and characteristics of points 0 to 4 are summarized in Table 1.

### 3. ANALYSIS

Phase plane, time response, and power spectral density of Mathieu equation for parameters at points 0 to 4 are plotted in Figure 4(a) to Figure 4(e), applying initial conditions  $x(0) = 1, \dot{x}(0) = 0$ . The powers are calculated based on fast Fourier transform algorithm over  $20\pi$  time response [12]. Time history responses are plotted for the first  $10\pi$  time units, while phase plane responses are showing for  $4\pi$  time units. In addition, the first four Poincare points are also indicated on the phase plane responses for shooting time  $T_p = \pi$ .

Figure 4(a) indicates that point 0 has a  $\pi$ -periodic response based on time response, Phase plane, and repeating Poincare points. In addition, power density designates a strong  $\pi$ -periodic spike as well as a  $(\pi/2)$ -periodic and  $(\pi/3)$ -periodic sub-harmonics. It also represents existence of a very long period super-harmonic. The power of  $\pi$ -periodic response is much higher than sub-harmonics, indicating that  $\pi$ -periodic response is the dominant period, but it is an asymmetric oscillation.

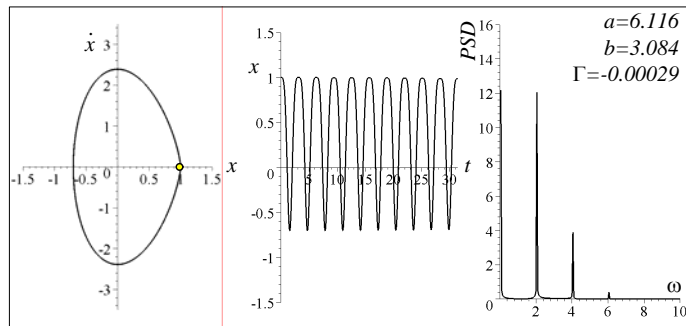


**Figure 4(a).** Phase plane, time response, and power of Mathieu equation of point 0 on path BC.

In Figure 4(b),  $a$  is 6.417 corresponding to the local minimum of Energy-Rate at point 1. The response of the system at this point is quasi-periodic response with an overall period very close to  $10\pi$  as indicated in phase plot

of the system. Point 2 at  $a=7.205$  corresponds to the  $4\pi$ -periodic ridge.

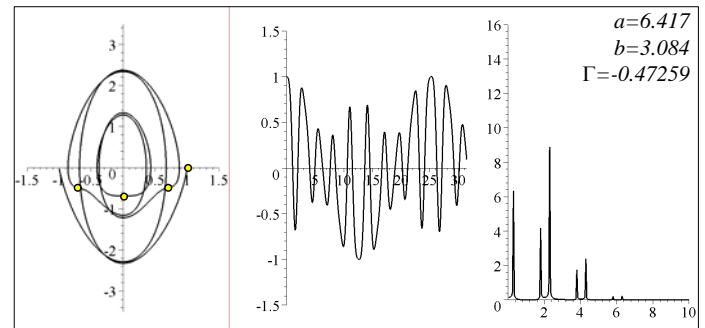


**Figure 4(b).** Phase plane, time response, and power of Mathieu equation of point 1 on path BC.

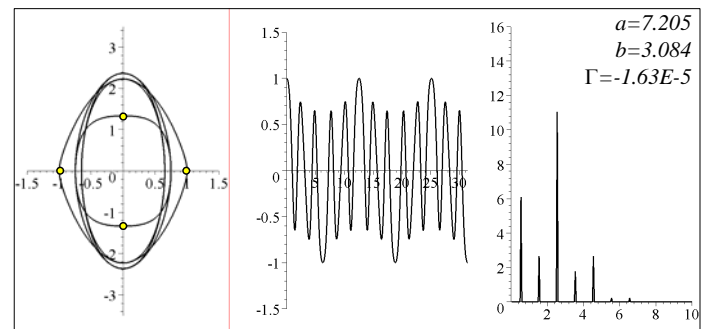


**Figure 4(c).** Phase plane, time response, and power of Mathieu equation of point 2 on path BC.

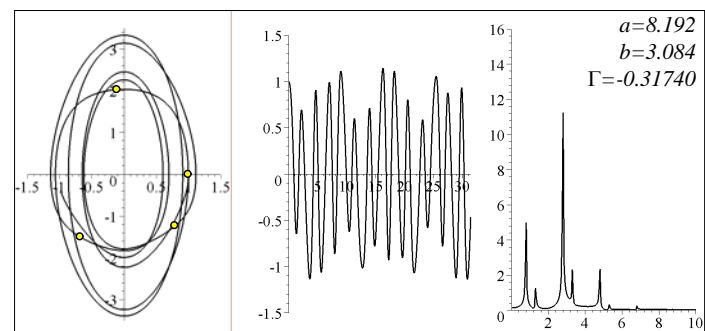
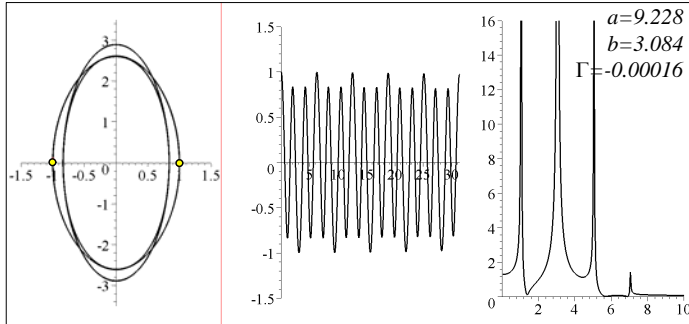


**Figure 4(d).** Phase plane, time response, and power of Mathieu equation of point 3 on path BC.

The  $4\pi$ -periodic response is obvious by investigating the phase plot, Poincare points, and time response of the system in Figure 4(c). At this point, the spikes of the power spectral appear exactly at points 0.5, 1.5, 2.5, 3.5, 4.5, 5.5, 6.5, which are corresponding to  $(4\pi)$ ,  $(4\pi/3)$ ,  $(4\pi/5)$ ,  $(4\pi/7)$ ,  $(4\pi/9)$ ,  $(4\pi/11)$ , and  $(4\pi/13)$  periods. The power of  $(4\pi)$ , and  $(4\pi/5)$  are stronger than the other sub-

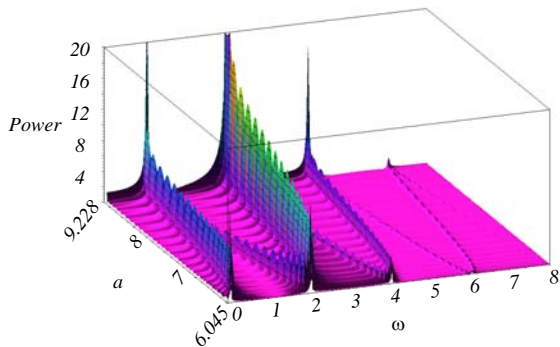
harmonics, while  $(4\pi/11)$ , and  $(4\pi/13)$  sub-harmonics are the weakest.

Figure 4(d) illustrates the behavior at the well  $w_I$ , and Figure 4(e) depicts response of the system at point 4 corresponding to  $2\pi$ -transition curve.



**Figure 4(e).** Phase plane, time response, and power of Mathieu equation of point 4 on path BC.

Investigating powers in Figures 4(a) to 4(e) presumes that by moving from  $\pi$ -transition curve to  $2\pi$ -transition curve, the period must gradually change from the period set  $\{(\pi), (\pi/2), (\pi/3), (\pi/4), \dots\}$  to the set  $\{(2\pi), (2\pi/3), (2\pi/5), (2\pi/7), \dots\}$ . Figure 5(a) depicts the power spectral density of Mathieu equation when the investigating point moves on line BC slowly. The resolution of the graph is 10000 points per unit  $a$ . It clearly shows the variation of super and sub harmonics of Mathieu equation in third stable region, for  $b=3.084$ , and  $6.116 < a < 9.228$ . It also indicates the power of sub-harmonics are much lower than the power of harmonics around  $(\pi)$ , and  $(\pi/2)$ . Projection of the power surface makes a two dimensional graph indicating the peak values of power on  $(a, \omega)$  plane, as shown in Figure 5(b).



**Figure 5(a).** 3-dimensional illustration of power spectral density of Mathieu equation in third stable region, for  $b=3.084$ .

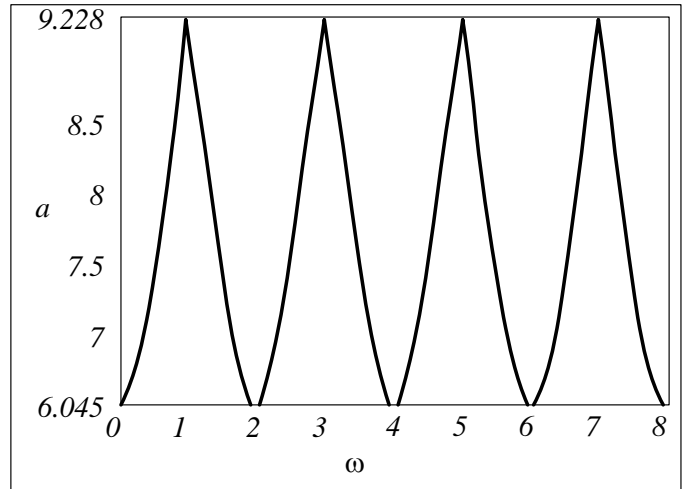


**Figure 5(b).** Top view of power spectral density surface of Mathieu equation in third stable region, for  $b=3.084$ .

Response of Mathieu equation for  $b=0$  must be a simple harmonic oscillation with a unique principal period equal to  $T = 2\pi / \sqrt{a}$ , while its response is periodic or quasi-periodic for  $b \neq 0$ . In order to investigate distribution of sub and super harmonics of Mathieu equation on transition curves and on a periodic ridge, we illustrate power spectral density of the equation on the lines AB, DC and EF of Figure 2 or 3. Line AB is on the  $\pi$ -periodic  $ce_2$  (cosine elliptic of second order), line DC is on the  $2\pi$ -periodic  $se_3$  (sine elliptic of third order), and line EF is on the  $4\pi$ -periodic ridge.

A 3-dimensional illustration of power spectral density of Mathieu equation on the  $\pi$ -transition curve, between points A and B is depicted in Figure 6. Obviously, the response of Mathieu equation at point A must be a pure  $\pi$ -periodic response with no sub or super harmonics. But when  $b \neq 0$ , sub and super harmonics appear, although  $a$  and  $b$  are set on a transition line. A unique and alone  $\pi$ -periodic response at point A is obvious in Figure 6. By moving from A toward B, a very long super-harmonic, and  $(\pi/2), (\pi/3), (\pi/4), \dots$ , sub-harmonics are appearing and growing. The power of  $\pi$ -periodic response is much higher than the other harmonics while  $b$  is sufficiently small. The power of  $\pi$ -periodic response has a negative rate, while the long super-harmonic and sub-harmonics have positive rates, indicating that participation of super and sub-harmonics are more at higher values of  $b$ .

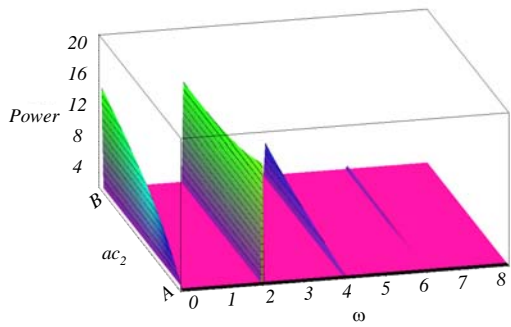


**Figure 6.** Three-dimensional illustration of power spectral density of Mathieu equation on the  $\pi$ -transition curve  $ce_2$ , between points A and B of Figure 3.

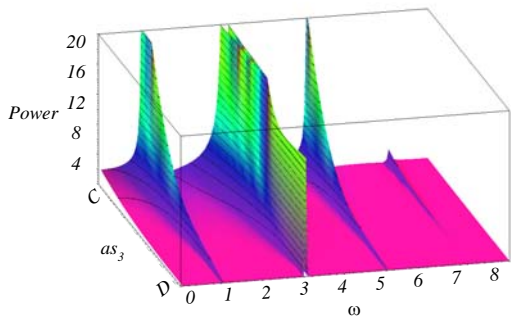


**Figure 7.** Three -dimensional illustration of power spectral density of Mathieu equation on the  $\pi$ -transition curve  $se_3$ , between points C and D of Figure 3.

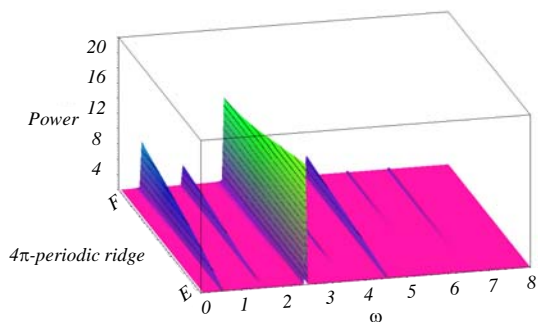


**Figure 14.** Three -dimensional illustration of power spectral density of Mathieu equation on the  $4\pi$ -periodic ridge, between points E and F of Figure 3.

A power spectral density on  $2\pi$ -transition curve, between points D and C is illustrated in Figure 7. Once again, the equation has a pure harmonic response with period  $T=2\pi/3$  at point D, but when we move toward point C, sub and super-harmonics are added to the response, as shown in Figure 7. Power spectral in Figure 7 also indicates that sensitivity of Mathieu equation to variation of  $a$  is getting higher at high values of  $b$ . In fact, detecting the transition curves of Mathieu equation at high values of both  $a$  and  $b$ , are not easy because of increasing sensitivity.

The first point E, of the  $4\pi$ -periodic ridge EF is at  $a=6.25$  providing a simple harmonic motion with period  $T=4\pi/5$ . By moving up, power spectral graph shown in Figure 8, show appearance of super and sub harmonics at  $(4\pi)$ ,  $(4\pi/3)$ ,  $(4\pi/5)$ ,  $(4\pi/7)$ ,  $(4\pi/9)$ ,  $(4\pi/11)$ , and  $(4\pi/13)$ . By increasing  $b$ , the power of  $4\pi$ -harmonic is growing faster than sub-harmonics, while the power of  $(4\pi/5)$ -harmonic has a decreasing trend.

## CONCLUSION

The third stable region of the Mathieu stability diagram has been investigated as an example of the stable regions. It is shown that the  $2\pi$ -periodic Energy-Rate surface shows one  $4\pi$ -periodic ridge as a coexistence splitting curve. The existence of super and sub-harmonics in quasi-periodic response of Mathieu equation has been analyzed on transition curves and on the  $4\pi$ -splitting curve of the third stable region, using power spectral density.

The Mathieu equation reduces to a simple harmonic oscillator with period  $T = \sqrt{a} = n$ ,  $n \in N$ , when  $b=0$ . For nonzero values of  $b$ , the response of Mathieu equation is quasi-periodic. When the values of  $a$  and  $b$  are such that the corresponding power plot indicates spike at  $\omega = m/k$ ,  $\{k, m\} \in N$ , then the point  $(a, b)$  is located on a periodic curve starting from  $a = \left(\frac{nk+m}{k}\right)^2$ ,  $\{k, m\} \in N$ ,  $k \geq 2$ ,  $m < k$ . The periodic curve is a transition curve, if  $k \bmod m$ , otherwise it is a splitting curve. The splitting curves have periods  $T=2k\pi/m$ .

## REFERENCES

1. McLachlan, N. W., (1947), *Theory and Application of Mathieu Functions*, Clarendon, Oxford U. P., Reprinted by Dover, New York, 1964.
2. Hayashi, C., (1964), *Nonlinear Oscillations in Physical Systems*, Princeton.
3. Alhargan, F. A., (1996), "A Complete Method for the Computations of Mathieu Characteristic Numbers of Integer Orders," *SIAM Review*, **38**(2), 239-255.
4. Whittaker, E. T., and Watson, G. N., (1927), *A Course of Modern Analysis*, Cambridge Univ. Press, 4th ed.
5. Van der Pol, B., and Strutt, M. J. O., (1928), "On the Stability of the solution of Mathieu's Equation", *The Philosophical Magazine*, vol. 5, p. 18.
6. Hill, G. W., (1886), On the part of the moon's motion which is a function of the mean motions of the sun and the moon, *Acta Math.*, **8**, 1-36.
7. Esmailzadeh E. and Nakhaie Jazar G., "Periodic Solution of a Mathieu-Duffing Type Equation", (1997), *International Journal of Nonlinear Mechanics*, **32**(5), p. 905-912,.
8. Cesari, L., (1964), *Asymptotic Behavior and Stability Problems in Ordinary Differential Equations*, Second Edition, Academic Press, New York, USA.
9. Ng, L., and Rand, R., (2002), "Nonlinear Effects on Coexistence Phenomenon in Parametric Excitation", *Proceeding of IMECE 2002, New Orleans, Louisiana, USA, November 17-22*.
10. Ng, L., R., Rand, and O'Neil, M., (2003), "Slow Passage Through Resonance in Mathieu's Equation", *Journal of Vibration and Control*, **9**, 685-707.
11. Nakhaie Jazar, G., (2004), "Stability Chart of Parametric Vibrating Systems, Using Energy Method", *International Journal of Nonlinear Mechanics*, **39**(8), 1319-1331.
12. Brigham, E. O., (1974), *The Fast Fourier Transform*, Prentice-Hall Inc., New Jersey,